Dynamics of Palmitic Acid Complexed with Rat Intestinal Fatty Acid Binding Protein[†]

Lingyang Zhu,[‡,§] Elizabeth Kurian,[||] Franklyn G. Prendergast,[||] and Marvin D. Kemple*[,‡]

Department of Physics, Indiana University Purdue University Indianapolis, Indianapolis, Indiana 46202-3273, and Department of Biochemistry and Molecular Biology, Mayo Foundation, Rochester, Minnesota 55905

Received August 27, 1998; Revised Manuscript Received November 25, 1998

ABSTRACT: Dynamics of palmitic acid (PA), isotopically enriched with ^{13}C at the second, seventh, or terminal methyl position, were investigated by ^{13}C NMR. Relaxation measurements were made on PA bound to recombinant rat intestinal fatty acid binding protein (I-FABP) at pH 5.5 and 23 °C, and, for comparison, on PA incorporated into 1-palmitoyl-2-hydroxy-*sn*-glycero-3-phosphocholine (MPPC) micelles, and dissolved in methanol. The ^{13}C relaxation data, T_1, and steady-state nuclear Overhauser effect (NOE) obtained at two different magnetic fields were interpreted using the model-free approach [Lipari, G., and Szabo, A. (1982) *J. Am. Chem. Soc. 104*, 4546−4559]. The overall rotational correlation time of the fatty acid·protein complex was 2.5 ± 0.4 ns, which is substantially less than the value expected for the protein itself (>6 ns). Order parameters (S^2), which are a measure of the amplitude of the internal motion of individual C−H vectors with respect to the PA molecule, while largest for C-2 and smallest for the methyl carbon, were relatively small (<0.4) in the protein complex. S^2 values for given C−H vectors also were smaller for PA in the MPPC micelles and in methanol than in the protein complex. Correlation times reflective of the time scale of the internal motion of the C−H vectors were in all cases <60 ps. These results support the view that the fatty acid is not rigidly anchored within the I-FABP binding pocket, but rather has considerable freedom to move within the pocket.

Palmitic acid (PA),[1] a 16-carbon fatty acid, binds with a stoichiometry of 1:1 and a dissociation constant of 4.1×10^{-8} M at 22 °C (*1*) to rat intestinal fatty acid binding protein (I-FABP). I-FABP is a monomeric, cytoplasmic protein which also binds several other saturated and unsaturated, long-chain fatty acids, and is a member of the family of intracellular lipid binding proteins (*2*, *3*). Although I-FABP appears to be involved in fatty acid transport as well as uptake, its overall role in cellular function has yet to be established. The three-dimensional structures of apo-I-FABP and of I-FABP complexed with several different fatty acids including PA have been determined by X-ray diffraction (*4*−*8*) and NMR (*9*, *10*). The protein consists of a single domain with 2 α-helices and 10 β-strands which form an overall β-barrel or β-clam motif as shown in Figure 1. Palmitic acid binds in a capacious cavity (or pocket) within the protein matrix. It is held within the pocket apparently by charge−charge interactions (ion pairing) of its negatively charged headgroup originating with the positively charged side chain of Arg-106 and by favorable van der Waal's interactions of the acyl chain with nonpolar amino acid side chains of the protein (*4*).

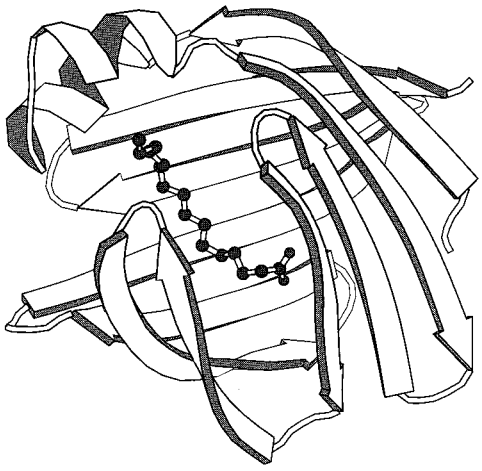

FIGURE 1: Ribbon diagram of I-FABP with a heavy atom rendering of bound palmitic acid based upon the X-ray crystal structure of the complex (*4*) prepared with the program MolScript (*40*).

The purpose of this work is to examine the effects of binding to I-FABP on the nanosecond and subnanosecond dynamics of palmitic acid. From NMR there is a great deal of information available on the dynamics of protein backbones, but less on the dynamics of protein side chains or on the influence of ligand binding on backbone and side chain dynamics (*11*, *12*, and references cited therein). To date there

[†] This work was supported in part by NIH Grant GM34847 to F.G.P.

* Corresponding author. E-mail: mkemple@iupui.edu.

[‡] Indiana University Purdue University Indianapolis.

[§] Present address: Department of Biochemistry and Molecular Biology, University of Chicago, Chicago, IL 60637.

[||] Mayo Foundation.

[1] Abbreviations: DSS, 2,2-dimethyl-2-silapentane-5-sulfonate; I-FABP, recombinant rat intestinal fatty acid binding protein; HMQC, heteronuclear multi-quantum correlation; MMPC, 1-myristoyl-2-hydroxy-*sn*-glycero-3-phosphocholine or lysomyristoylphosphatidylcholine; MPPC, 1-palmitoyl-2-hydroxy-*sn*-glycero-3-phosphocholine or lysopalmitoylphosphatidylcholine; NMRD, nuclear magnetic relaxation dispersion; NOE, steady-state (hetero)nuclear Overhauser effect; PA, palmitic acid; 1D, one-dimensional.

10.1021/bi982087v CCC: $18.00
Published on Web 01/14/1999

is almost no information on the influence of binding on the dynamics of the ligands themselves (*13*). The expectation is that ligand mobility should decrease substantially upon complexation with the protein inasmuch as the bound ligand is expected to be confined by the protein matrix. Interestingly, a more rigid, bound ligand would impose an entropic penalty on the free energy of binding; however, a rigidified ligand presumably would optimize subsequent enzymatic action. Such reasoning for the complex of I-FABP with a fatty acid molecule suggests that the internal motions of the fatty acid bound to I-FABP would be restricted when compared with the fatty acid free in solution, and further that there likely would be differences in the amplitude of internal motion with position along the aliphatic chain of the fatty acid due to specific interactions between the protein and the bound fatty acid and due to the tendency for fatty acids to be more flexible toward the methyl end of their acyl chains when the headgroup is anchored (*14*, *15*).

To determine if the above predictions bear out, we have probed the dynamics of PA complexed with I-FABP using ^{13}C NMR relaxation rate measurements made on PA enriched separately at the 2-, 7-, and 16- (methyl) positions with ^{13}C. Comparisons of the dynamics were made with the fatty acid complexed with I-FABP and lysopalmitoylphosphatidylcholine (MPPC) micelles, and free in a methanol solution. Relaxation measurements were performed using direct detection of the ^{13}C signals to minimize complications due to cross-correlation of the carbon−proton magnetic dipolar interactions at the specific sites in the fatty acid.

MATERIALS AND METHODS

Palmitic acid, isotopically enriched with ^{13}C either at the 2-position or at the terminal methyl position, was purchased from Cambridge Isotope Laboratories, Inc. (Andover, MA). Palmitic acid labeled at the 7-position with ^{13}C was synthesized specially for these experiments by Molecular Probes, Inc. (Eugene, OR). Recombinant I-FABP from rat intestine was expressed and purified as described by Kirk et al. (*16*), and protein solutions were prepared at pH 5.5 buffered with 20 mM potassium phosphate. Ligand·protein complexes were obtained as follows: ^{13}C-labeled PA was dissolved in chloroform, and a low stream of nitrogen gas was used to dry the PA into a thin film on the inside surface of the tube originally containing the mixture. A solution of I-FABP at a concentration <100 μM then was added to the tube containing the fatty acid film in an amount slightly in excess of the amount of fatty acid and stirred for 24 h. Finally, this solution was concentrated to reach an I-FABP concentration of $\sim$1.8 mM which was determined by UV absorption using an ϵ_{280} of 18 700 M^{-1} cm^{-1} for I-FABP (*16*). The samples also contained 10% D_2O for locking the magnetic field in the NMR experiments. An identical procedure was followed to form the complexes of I-FABP with each of the three ^{13}C-labeled forms of PA. In no case was there any indication of precipitate in the preparations.

MPPC was purchased from Avanti Polar Lipids (Birmingham, AL) in powdered form. The powder was dissolved into a 20 mM aqueous phosphate solution at pH 5.6 or 7.1 containing 10% D_2O. ^{13}C-labeled PA was dissolved in methanol and was dried by nitrogen gas in a manner similar to that described for the I-FABP complexes above, and the solution containing MPPC was added. To ensure the formation of micelles, ultrasonication was performed for 30 min on the final solution consisting of 2 mM palmitic acid and 40 mM MPPC. This procedure was followed for 2-^{13}C- and methyl-^{13}C-labeled PA. Finally, as a third example of fatty acid dynamics, unlabeled PA was dissolved into perdeuterated methanol (CH_3OD) at a concentration of 50 mM.

Table 1: ^{13}C T_1 and NOE of Palmitic Acid[a]

	125.6 MHz		75.4 MHz	
position	T_1 (s)	NOE	T_1 (s)	NOE
		I-FABP Complex[b]		
2	0.30 ± 0.01	1.54 ± 0.08	0.15 ± 0.01	1.49 ± 0.08
7	0.30 ± 0.02	1.99 ± 0.10	0.19 ± 0.01	1.95 ± 0.10
methyl	1.27 ± 0.06	2.56 ± 0.13	1.03 ± 0.05	2.46 ± 0.12
		MPPC Micellar Complex[c]		
2	0.49 ± 0.02 (0.49 ± 0.03)	2.27 ± 0.11 (2.26 ± 0.11)	0.36 ± 0.01 (0.37 ± 0.02)	2.26 ± 0.09 (2.25 ± 0.11)
methyl	−	−	2.37 ± 0.10	2.66 ± 0.13
		In Methanol[d]		
2	1.92 ± 0.10	2.22 ± 0.22	1.87 ± 0.09	2.28 ± 0.23
3	1.89 ± 0.10	2.24 ± 0.22	1.80 ± 0.09	2.30 ± 0.23
7	1.80 ± 0.09	2.93 ± 0.15	1.70 ± 0.09	2.85 ± 0.14
methyl	5.8 ± 0.5	−	5.7 ± 0.3	−

[a] Data that are not available are denoted by "−". [b] Palmitic acid concentration, 1.6 mM; pH, 5.5; temperature, 25 °C. [c] Palmitic acid concentration, 2 mM; MPPC concentration, 40 mM; temperature, 25 °C; pH, 5.6. pH 7.1 results are given in parentheses. [d] Palmitic acid concentration, 50 mM; temperature, 25 °C.

NMR experiments were performed on Varian Unity 300 and 500 MHz spectrometers (at IUPUI). The samples were maintained at 23 °C (for the I-FABP complex) or 25 °C (for the MPPC complex and the fatty acid/methanol solution) during data acquisition. ^{13}C chemical shifts were measured with respect to external dioxane at 69.3 ppm relative to DSS and were reproducible within ±0.05 ppm. ^{13}C T_1 values were measured at 75.4 and 125.6 MHz with direct detection using a standard inversion−recovery pulse sequence with 12 (different) delay times. Proton decoupling was performed during the relaxation delay period and during acquisition using a Waltz-16 pulse sequence (*17*). Proton decoupling in the T_1 experiments eliminates effects from cross-relaxation, interference between chemical shift and dipolar interactions (*18*), and dipolar cross-correlations in a CH_2 group (2-^{13}C and 7-^{13}C) which is an AMX system (*19*). Effects of dipolar cross-correlation on methyl T_1 and NOE values were minimized by following suggestions of Kay and Torchia (*20*) and by extracting T_1 values from magnetization recoveries out to delay times $\leq 3T_1$ only. The recycle time in the T_1 measurements was at least 4 s. The steady-state NOE was obtained by collecting ^{13}C 1D spectra alternately with and without ^{1}H saturation with a recycle time of 6 s.

Vnmr 4.3 software (Varian) was used for NMR data reduction. Normally, 8K data points were zero-filled to 16K points before Fourier transformation. Exponential apodization corresponding to a line broadening of 2−5 Hz was applied. T_1 values were obtained by three-parameter fits of signal peak heights at different relaxation delay times to a single-exponential function. The final values of T_1, given in Table 1, typically are averages of values determined from 2−3 independent experiments. The uncertainties in the T_1 values (estimated normally to be on the order of ±5%) were determined from the reproducibility of the values and the

quality of the fitting of the recovery curves. NOE was calculated as the ratio of ^{13}C signal intensities obtained with and without proton saturation. The intensities were measured from both peak heights and peak areas, and consistent results were obtained. The mean NOE values and their standard deviations (also generally around ±5%) were calculated based typically upon 3−4 independent measurements.

In these experiments, relaxation of the ^{13}C magnetization is due to the magnetic dipolar interaction between the ^{13}C nucleus and the attached protons with a considerably smaller contribution from the chemical shift anisotropy (CSA) interaction. The appropriate equations for T_1 and NOE are given in the literature (see, for example, refs *21* and *22*). Molecular motion enters the problem through the frequency-dependent spectral density, $J(\omega)$; therefore, interpretation of the relaxation data in terms of molecular motion rests on the choice of the form of the spectral density. Here we make use of the model-free formalism of Lipari and Szabo (*23*). The utility of this approach is that specific models for the motion are not required. Rather, the appropriateness of a given motional model can be determined by comparison of motional parameters predicted by the model with parameters derived from the data using the Lipari and Szabo spectral density (*23*):

$$J(\omega) = {}^{2}/_{5}\left[\frac{S^2\tau_m}{1+\omega^2{\tau_m}^2} + \frac{(1-S^2)\tau}{1+\omega^2\tau^2}\right] \quad (1)$$

where τ_m is a correlation time representing the overall rotational motion of the molecule, S^2 is the generalized order parameter, and τ_e is an effective correlation time for the internal motion of the C−H vector found from $\tau^{-1} = {\tau_m}^{-1} + {\tau_e}^{-1}$. Of the motional parameters, τ_m is a global parameter, and τ_e and S^2 are local parameters.

Modifications of $J(\omega)$ in eq 1 are available including the addition of various parameters to deal with the possibility of anisotropic overall rotational motion (*24*) and the addition of order parameters and correlation times to account for internal motion that is not in the NMR motional narrowing limit (*25*). In this work, we have taken the overall motion to be isotropic (see below), and we have followed the procedure outlined by Mandel et al. (*21*) to settle on the optimum number of parameters for the internal motion and to determine their values based upon least-squares fits of the relaxation data to the applicable equations using the program Modelfree 3.1 written by Arthur Palmer of Columbia University (*21*). The overall quality of the fits was assessed from $\chi^2 = (N - N_P)^{-1}\sum_{i=1}^{N}(m_i - c_i)^2/\sigma_i^2$ with N, the total number of data, N_P, the total number of fitting parameters, m_i and c_i, the measured and calculated values of the relaxation quantities, respectively, and σ_i, their estimated uncertainties, and by fits of data sets generated from Monte Carlo simulations (500 in each case). The quoted uncertainties in the motional parameters were derived from fits of the simulated data generated by Modelfree 3.1. A value of 40 ppm was used for the strength of the CSA for all sites based upon typical values for aliphatic ^{13}C nuclei generally (for example, see ref *26*). Any variation present in the CSA from site to site in the molecules has a negligible effect on the fitting results since the CSA contributes <1% to the relaxation rates of methylene and methyl carbons at the magnetic fields of this study.

Table 2: Motional Parameters of Palmitic Acid in I-FABP and MPPC Micelles

position	S^2	τ_e (ps)	S^2_{Axis} [a]	α (deg) [b]
I-FABP Complex, $\tau_m = 2.5 \pm 0.4$ ns, $\chi^2 = 0.91$				
2	0.37 ± 0.03	26 ± 6		45
7	0.21 ± 0.02	54 ± 5		55
methyl	0.014 ± 0.003	10 ± 1	0.13 ± 0.02	61
MPPC Micellar Complex, $\tau_m = 1.4 \pm 0.4$ ns, $\chi^2 = 2.4$ [c]				
2	0.084 ± 0.008	35 ± 3		65
	(0.089 ± 0.010)	(31 ± 3)		
methyl	0.004 ± 0.001	5 ± 1	0.03 ± 0.01	74

[a] S^2_{Axis} is the order parameter of the C-15−C-16 bond. [b] Calculated from the Kinosita model. [c] Values for pH 7.1 are in parentheses ($\tau_m = 1.0 \pm 0.3$ ns, $\chi^2 = 0.53$).

RESULTS AND DISCUSSION

The measured ^{13}C chemical shifts (relative to DSS) at positions 2, 7, and 16 of PA in I-FABP were 39.5, 32.0, and 16.7 ppm, respectively (±0.05 ppm). In the other "solvents", the ^{13}C chemical shifts were 37.1 and 36.0 ppm for C-2 of PA in the MPPC complex and in methanol, 32.7 ppm for C-7 of PA in methanol, and 15.8 and 15.5 ppm for C-16 of PA in MMPC and methanol. T_1 and steady-state NOE data for those carbons and for C-3 of PA in methanol are presented in Table 1, and the corresponding motional parameters derived from the relaxation data are listed in Table 2. In addition to τ_m, S^2, and τ_e, the parameter, S^2_{Axis} is listed in Table 2 for the methyl group (C-16). S^2_{Axis} is derived from a motional model generally applicable to methyl groups (*27*). In the model, the motion of each of the three methyl C−H vectors is taken to be identical and axially symmetric about the C−C bond between C-15 and C-16 in PA. Tetrahedral geometry is assumed with each C−H vector maintaining a fixed angle of 70.5° with the C−C bond. S^2 then is a product of two order parameters according to $S^2 = (1/9)S^2_{Axis}$ and S^2_{Axis} represents the motion of the C−C bond. To assess flexibility along an acyl chain in general, ideally one would compare order parameter values for C−C bonds. However, at methylene positions, the C−H S^2 does not factor into two other order parameters because the motion of the C−H vectors is unlikely to be axially symmetric, at least not about a C−C bond. The methylene results thus are expressed as a single order parameter, that order parameter reflecting the motion of the two C−H vectors of the given methylene which we take to be the same. We are left with imperfect comparisons, but it is clearly more sensible to compare S^2_{Axis} for a methyl group—and not its measured S^2 value—with the order parameters for the other sites. In the sections that follow, we first discuss the results for each sample followed by a comparison of the results over the range of samples.

Palmitic Acid·I-FABP Complex. These results are the primary focus of this paper. As noted, PA binds tightly ($K_d \sim 40$ nM, ref *1*) in the cavity of I-FABP at a stoichiometry of 1:1, and we expect binding to influence its dynamics. For the three sites probed in the bound palmitic acid, three motional parameters, τ_m, S^2, and τ_e, proved to be both necessary and sufficient to fit the T_1 and NOE data. The S^2 value of 2-^{13}C (0.37, Table 2) indicates that the fatty acid

headgroup is not completely immobilized in the protein, and in fact that it has considerable freedom of internal motion. The internal motion is noticeably different at the two ends of the chain as noted by the difference in S^2 for C-2 and S^2_{Axis} for C-15−C-16. The ordering of order parameter values along the chain, S^2(C-2) > S^2(C-7) > S^2_{Axis}(C-16), is consistent with the structure of the fatty acid and the general expectation that the headgroup serves as a primary locus of the interaction of the fatty acid and the protein. The τ_e values, all of which are in the motional narrowing limit, appear to be reasonable and indicate that the time scale of the internal motion at the labeled positions in the fatty acid has an upper bound of ~60 ps. The τ_e values for the CH_2 groups are similar in size to those observed for the 26-residue peptide melittin as a monomer in solution (*22*) and are of similar to somewhat larger size than values typically found for protein backbone vectors, many of which are taken to be zero (*21*, *28*). A correlation between motional freedom as reflected in the order parameter and τ_e appears to exist in general for non-methyl C−H vectors. Specifically, τ_e tends to be larger when S^2 is smaller.

The unexpected result is the τ_m value. Both published (*29*) and unpublished (Zhu, L., Kurian, E., Prendergast, F. G., and Kemple, M. D., in preparation) ^{15}N relaxation studies of the dynamics of the backbone of I-FABP have given a correlation time for the overall rotation of holo-I-FABP of 6.2 ns, a number consistent with the size of I-FABP. Similar values (6−7 ns) were derived from NMRD (Wiesner, S., Kurian, E., Prendergast, F. G., and Halle, B., *J. Mol. Biol.*, in press) and fluorescence anisotropy decay measurements (*30*; and Klimchuk, E., Kurian, E., Kirk, W. R., and Prendergast, F. G., unpublished information). The smaller τ_m value found in the present work appears to indicate that the fatty acid is not anchored tightly within the protein binding cavity, but rather that it is undergoing "segmental motion" within the cavity. This view can be reconciled with the standard Lipari and Szabo formalism (*23*) in the following way.

The autocorrelation function describing the motion of a C−H vector in the bound fatty acid, $C(t)$, is written as a product of three terms representing independent motion on three different time scales according to

$$C(t) = C_O(t)C_S(t)C_I(t) \tag{2}$$

where the subscripts O, S, and I refer to the overall rotational motion (O) of the complex, a segmental motion (S) of the entire fatty acid molecule or some fraction of it within the binding cavity occurring on a time scale intermediate to that of the overall motion, and the subnanosecond internal motion (I) of the vector with respect to the fatty acid. After Lipari and Szabo (*23*), we write

$$C_O(t) = \frac{1}{5}\exp(-t/\tau_m)$$

$$C_S(t) = S_S^2 + (1 - S_S^2)\exp(-t/\tau_S)$$

$$C_I(t) = S^2 + (1 - S^2)\exp(-t/\tau_e) \tag{3}$$

where τ_m, S^2, and τ_e have their usual meaning, and S_S^2 and τ_S are, respectively, the order parameter and correlation time for the segmental motion subject to the conditions, $0 \le S_S^2 \le 1$ and $\tau_e < \tau_S < \tau_m$. The segmental motion is restricted to the extent that S_S^2 differs from zero.

The spectral density derived from eq 3 is the sum of four terms:

$$J(\omega) = \frac{2}{5}\left[\frac{S_S^2 S^2 \tau_m}{1+\omega^2\tau_m^2} + \frac{S_S^2(1-S^2)\tau}{1+\omega^2\tau^2} + \frac{S^2(1-S_S^2)\tau_{meff}}{1+\omega^2\tau_{meff}^2} + \frac{(1-S_S^2)(1-S^2)\tau_{eff}}{1+\omega^2\tau_{eff}^2}\right] \tag{4}$$

In this equation, $\tau_{meff}^{-1} = \tau_m^{-1} + \tau_S^{-1}$, $\tau^{-1} = \tau_m^{-1} + \tau_e^{-1}$, and $\tau_{eff}^{-1} = \tau_m^{-1} + \tau_S^{-1} + \tau_e^{-1} = \tau_{meff}^{-1} + \tau_e^{-1}$. The spectral density in eq 4 clearly has too many parameters for the number of data available, but by making some reasonable simplifications, we can gain some physical insight. First, we assume that S_S^2 is close to zero or, in other words, that the motion of the segment in question is nearly unrestricted. This assumption coupled with the observations that normally $(\omega\tau_m)^2 \gg 1$ and τ_e is $\ll \tau_m$ allows the first two terms in eq 4 to be neglected (provided T_2 data are not used). Then replacing $(1 - S_S^2)$ by Q^2 we have

$$J(\omega) = \frac{2}{5}Q^2\left[\frac{S^2\tau_{meff}}{1+\omega^2\tau_{meff}^2} + \frac{(1-S^2)\tau_{eff}}{1+\omega^2\tau_{eff}^2}\right] \tag{5}$$

which has exactly the form of the spectral density proposed to take internal motions into account that are not in the motional narrowing limit (*25*). The parameters in eq 5 have different meanings from those in the spectral density of ref *25*, however. In particular, Q^2, which should be near 1, is a measure of the loss of order due to the motion of the segment; the larger Q^2 is, the larger the amplitude of the segmental motion. Also τ_{meff} ($<\tau_m$ and τ_S) depends on the correlation time for the segment and could be $\sim\tau_S$ depending on how much τ_S differs from τ_m. S^2 and τ_e have their normal interpretation in reference to the subnanosecond local motions within the segment. This approach can be applied in its simplest form (eq 5) using the program Modelfree (*21*). The parameter τ_{meff} replaces the overall correlation time given by the program, and Q^2 replaces S_f^2. S^2 and τ_e are unchanged and can be identified with the Modelfree parameters depending on the number of parameters included in the fitting procedure. Since τ_{meff} depends on both τ_m and τ_S, an independently known value for τ_m is required to find τ_S.

The optimum fitting of the relaxation data for the PA·I-FABP complex occurred for $Q^2 = 1$. When we allowed Q^2 to differ from 1 in a four-parameter fit also including τ_{meff}, τ_e, and S^2, which was feasible because four pieces of relaxation data were available for each position, the data were not described by the resulting parameters significantly better statistically than by the standard three parameters ($Q^2 = 1$). If the fatty acid as a whole is taken to be the segment, our result implies that the fatty acid moves sufficiently freely within the binding cavity such that the corresponding order parameter S_S^2 is ~0. In turn, the value listed for τ_m in Table 2 for the PA·I-FABP complex becomes τ_{meff} in this model. So, using 2.5 ns from Table 2 for τ_{meff} and 6.2 ns for τ_m (from above), we find $\tau_S = 4.2$ ns. While the apparent angular amplitude of the segmental motion of the fatty acid

within the cavity is relatively large, the time scale of the motion is much longer than is found for free fatty acid (see below). The amplitude of the internal motion inferred from the S^2 values is, however, reduced in the protein complex relative to the free fatty acid (again, see below). Note that the segment in this analysis is not necessarily the fatty acid as a whole, but could just as well consist of elements of the fatty acid including the C−H vectors examined. Effective segmental rotations of the methylenes along the fatty acid chain then would have the effect of reducing the overall correlation time extracted.

This model presents a rationale for the observation of an overall correlation time that is smaller than that of the holoprotein itself and yields a value for the time scale of the segmental motion of the bound PA under the assumptions that the segmental and overall motions are independent. Although the latter assumption cannot be rigorously correct, the model nonetheless does give insight into the nature of the dynamics of the bound ligand. Equation 5 has potential applications to aid in interpreting the dynamics of ligand binding in general and the dynamics of partially or completely unfolded proteins depending on the time scales of the motion.

One question that needs to be addressed is whether the smaller than expected effective overall rotational correlation time derived from the data is an artifact, due either to experimental factors or to aspects of the data analysis. For example, the presence of palmitic acid free in solution could give misleading results since free fatty acid would have a shorter overall rotational correlation time such as we found for palmitic acid in methanol (see below). However, this concern can be ruled out for several reasons. First, PA binds extremely tightly to I-FABP, $K_d = 41$ nM (*1*), and the samples were prepared in such a way as to ensure fully bound fatty acid. Second, PA has extremely low solubility in aqueous solution. Even if there were unligated PA present, its concentration in solution would be below detectable limits by NMR unless the fatty acid were micellized. However, given the final concentrations of PA, if there were sufficient PA available to form micelles, the micelles should have been evident. Finally, only one set of signals from ^{13}C and from attached ^1H nuclei was observed in experiments with a given ^{13}C-labeled palmitic acid, and it is highly unlikely that bound and free fatty acids would have identical chemical shifts.

Another potential complicating factor, discussed briefly in earlier sections, is that cross-correlation originating from the two C−H dipolar interactions in the case of both C-2 and C-7 could lead to errors in the measured T_1 and NOE values. However, Zhu et al. (*19*) demonstrated that there is no contribution of dipolar cross-correlation to T_1 and NOE if the particular CH_2 group is an AMX system (proton−proton scalar coupling constant small compared with the chemical shift difference of the two proton resonances), and that errors in T_1 and NOE are <10% even for AX_2 systems for most motional models tested. For the palmitic acid·protein complex, signals from the two protons attached to C-2 and to C-7 of PA are separated by 0.6 and 0.2 ppm, respectively, as shown in Figure 2. Since the proton−proton scalar coupling constant is ~20 Hz, both C-2 and C-7 satisfy the AMX criterion at 300 and 500 MHz. Zhu (unpublished results) demonstrated further that errors in T_2 measurements readily exceed 10% for AX_2 *and* AMX systems, giving a

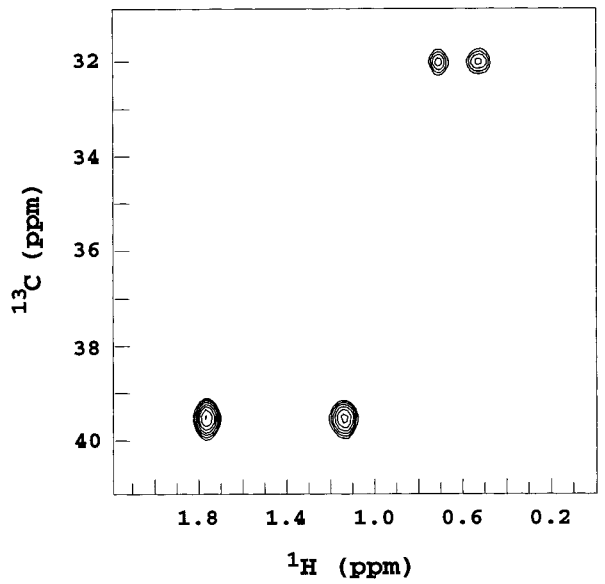

FIGURE 2: $^{13}C-^1H$ HMQC spectrum at 11.1 T and at 25 °C (with ^{13}C decoupling during acquisition) of ^{13}C-2 palmitic acid and ^{13}C-7 palmitic acid complexed with I-FABP at pH 5.5 in 20 mM phosphate buffer. The spectrum consists of signals superimposed with the same frequency scales from two different samples, one containing ^{13}C-2 palmitic acid (signals lower left) and one with ^{13}C-7 palmitic acid (signals upper right). ^{13}C chemical shifts are referenced to DSS at 0 ppm (see text) and ^1H chemical shifts to water at 4.76 ppm.

powerful reason for not including T_2 values in the analysis of these data. Last, it should be noted that ^{13}C T_1 and NOE data from methylene groups in glycine and from methine groups of other amino acid residues in monomeric, tetrameric, and micelle-bound melittin gave consistent τ_m values (*22*, *26*).

In all of these kinds of dynamic studies, there is always concern regarding the validity of the motional parameters. Here the parameters were derived from the relaxation data by fitting the T_1 and NOE data for C-2, C-7, and C-16 together. Significantly, nearly the same parameters were obtained from individual fits for C-2 and C-7. (S^2 is too small for it to be feasible to find τ_m from the data for C-16.) Fits of the relaxation data in which τ_m was fixed at 6.2 ns were inferior to those in which τ_m was optimized, the former having a χ^2 of 2.2 vs 0.91 for the latter (Table 2), and application of the criteria outlined by Mandel et al. (*21*) showed that treating τ_m as a parameter to be optimized gave a statistically significant, superior result. Similarly, adding an additional order parameter did not lead to improved fitting of the data as noted above.

Regarding the issue of anisotropic motion, I-FABP is itself nearly spherical (*4*−*10*). Treating deviations to first order by approximating I-FABP as a cylindrical protein, one finds that the ratio of long and short axis lengths is ≤1.2. This degree of anisotropy could in no way account for the observation of a τ_m that is more than a factor of 2 smaller than the expected value. In terms of the segmental motion model, on the other hand, it is conceivable that PA moves anisotropically within the binding cavity, a situation which might cause some error in the S^2 values. However, there are not enough data available nor is there a sufficient theoretical foundation to justify adding parameters to attempt to account for that possibility, and in any event, the inference that PA

is able to move relatively freely within the pocket would still be valid. In summary, the finding of a smaller overall effective correlation time than expected for the fatty acid·protein complex appears to be robust.

Palmitic Acid in MPPC Micelles. Relaxation measurements were also made for PA in MPPC micelles for comparison with the protein complex. MPPC was chosen as the micelle matrix for the following reasons. (1) It has a very low critical micelle concentration (7 μM, ref *31*). Thus, at the 40 mM MPPC concentration used in these experiments, the lipid should be dispersed in the form of micelles only. (2) The hydrophobic tail of MPPC is the same length as the acyl chain of palmitic acid, bolstering the assumption that palmitic acid when added in the ratio of 1:20 [PA]:[MPPC] would not perturb the micelle structure in any significant fashion. Presumably the fatty acid molecules position themselves inside the micelles with their carboxylate groups near the surface and their hydrocarbon tails toward the center of the micelles, parallel to the fatty acyl chains of the MPPC. (3) The MPPC micelles, or more precisely MPPC/PA mixed micelles, should be nearly spherical in solution, satisfying the condition of isotropic overall motion in eq 1.

Relaxation data for C-2 and the methyl carbon of palmitic acid are given in Table 1. T_1 at a given frequency for a given carbon was smaller than the corresponding value in methanol, but larger than those in the protein complex. An HMQC spectrum collected at 500 MHz of PA in the MPPC micelle showed the two proton signals of C-2 to be separated by 0.27 ppm, indicating that the AMX criterion discussed above is satisfied. The motional parameters derived from the relaxation data are included in Table 2. No significant differences were present at the two pH values used.

The τ_m value of ~1 ns is smaller than expected based upon previous work involving MMPC micelles and estimates of the size of the micelles (*26*). This result likely reflects the fact that the micelles are quite "fluid" and that PA moves within the micelle. Both rotation about its long axis and lateral diffusion of PA "around" the micelle will contribute to the ^{13}C relaxation in the acyl chains and effectively reduce the value of τ_m that satisfies the data relative to the value that would be appropriate for a rigid body the size of the micelles.

Palmitic Acid in Methanol. Nine resonances were resolved in the natural-abundance ^{13}C NMR spectrum of PA in methanol. Assignments were made by comparison of the ^{13}C chemical shifts in methanol with those in the I-FABP and MPPC complexes, and from the behavior of the ^{13}C relaxation rates along the acyl chain of PA (*32*). T_1 and NOE values (Table 1) increased generally toward the methyl end of the chain due to increasing mobility which may in part be due to self-association of the fatty acid known to occur in aprotic solvents at concentrations above ~10 mM (*33*). τ_m was not well-defined by the data, and as a result, motional parameters for PA in methanol are not included in Table 2. This outcome is likely due to two factors. First, the overall motion of palmitic acid in solution is presumably highly anisotropic, and an adequate description of the motion would require additional parameters (*24*). Second, the analysis yielded a range of τ_m values (~0.1−0.8 ns) that generated reasonable fits of the data, and in every case S^2 at each site was near 0, consistent with the observed insensitivity of the data to τ_m.

Dynamic Comparisons. The most restricted internal motion of PA as indicated by S^2 values occurred in the protein complex with yet smaller values found for the same carbon positions for PA in the micellar complex and in methanol. By no means, however, is the motion very restricted. For example, the largest S^2 value (C-2, 0.37) in the PA·I-FABP complex is small compared with those typical of N−H vectors in protein backbones (see references included in *11*) and smaller than Cα−H S^2 values that we measured in the interior of an unstructured peptide (*22*). The structure of holo-I-FABP (*4*) indicates that the headgroup of the bound fatty acid interacts electrostatically with the protein side chain of Arg-106, the latter being about two-thirds of the way into the binding cavity relative to the putative entrance to the cavity. The fatty acid's acyl chain bends, leaving the methyl group located in the vicinity of the entrance (Figure 1). Judging from this structure, internal motions in the PA·I-FABP complex apparently are partially restricted by interactions of the headgroup with the protein and by constraints placed on the acyl chain by other protein side chains. The observation that S^2 for C-2 was larger than that for C-7 is consistent with the primary site of interaction of the fatty acid involving the headgroup, and with the general pattern of dynamics along an extended acyl chain (*14*, *34*−*36*, and results found here in the other systems). The small value for S^2_{Axis} at the PA terminus presumably also reflects both the motional freedom allowed at this position by the protein and the tendency for the methyl end of the acyl chain to show the most motion anyway. The ordering of S^2 values also coincides with the ordering of *B*-factors derived from the X-ray diffraction studies of the structure of the PA·I-FABP complex (*4*). In particular, *B*(C-2) < *B*(C-7) < *B*(C-16), consistent with increasing mobility down the acyl chain. In addition, the *B*-factors (*4*) are fairly large (19, 25, and 51 Å^2) in keeping with the relative motional freedom we find here of the bound fatty acid. The small τ_e values (<60 ps) observed in all cases indicate clearly that there are rapid internal motions all along the fatty acid acyl chain.

Motional Models. Order parameter values can be used to gain an idea of the angular amplitude of the internal motion by application of specific motional models. In this case, the most straightforward and reasonable model to apply is that proposed originally by Kinosita (*37*) in which the vector of interest is confined to a cone of half-angle α centered on the vector's equilibrium position and is equally likely to point in any direction within the cone. The order parameter, either S^2 for the methylenes or S^2_{Axis} for the methyl groups, equals $(1/4)\cos^2\alpha(1 + \cos\alpha)^2$. Cone angles derived from the measured order parameters are included in the last column of Table 2 where larger angles correspond to smaller order parameter values. In all cases, the Kinosita model indicates that the C−H vectors at the sites examined sample a considerable angular range with respect to a coordinate frame fixed in the fatty acid.

Motion of Palmitic Acid within the Protein Pocket. The marked disparity between the expected τ_m for a molecule the size of I-FABP [~6 ns from application of the Stokes−Einstein formalism which is consistent with 6.2 ns recovered from NMR relaxation measurements on the protein (*29*; and Zhu, L., Kurian, E., Prendergast, F. G., and Kemple, M. D., in preparation) and 6−7 ns recovered from NMRD (Wiesner,

S., Kurian, E., Prendergast, F. G., and Halle, B., *J. Mol. Biol.*, in press) and fluorescence anisotropy decay measurements (*30*; and Klimchuk, E., Kurian, E., Kirk, W. R., and Prendergast, F. G., unpublished information)] and that found in this study clearly must be related to the mobility of the protein-bound ligand. We have noted from past work that NMR-relaxation-determined τ_m values tend to be higher than those found from fluorescence anisotropy decay data for the same protein or peptide examined under similar physical conditions (*22*, *38*), in contrast to the situation here. Because the affinity constant for fatty acid binding to I-FABP is so large, one may be tempted to assume *a priori* that the ligand is well ensconced in a tightly packed, sterically complementary binding pocket. To rationalize the data we have presented, however, requires that the entire fatty acid be capable of substantial local motion within the pocket, admittedly less toward the carboxylate end but marked from the middle of the fatty acyl chain toward the tail with the terminal methyl group being almost totally unfettered. This inference seems inherently reasonable given how capacious the binding cavity is in I-FABP; depending on precisely how the cavity volume is calculated, it is at least twice the van der Waals's value of PA itself (Likić, V., and Prendergast, F. G., submitted). Additionally, the fatty acyl chain is not held in place by any specific interactions. Last, the volume in the cavity not occupied by the fatty acid, at least as assessed from the X-ray crystal structure, is filled with water molecules (*3*−*8*). The latter have been shown by MD simulation (Likić, V., and Prendergast, F. G., submitted) and NMRD measurements (Wiesner, S., Kurian, E., Prendergast, F. G., and Halle, B., *J. Mol. Biol.*, in press) to be in fast exchange with bulk water surrounding the protein. All of this implies relative freedom for the fatty acyl chain to bounce around in the pocket and raises interesting and obvious questions regarding the molecular basis underlying protein−ligand recognition and the measured high affinity of PA binding. Interestingly, if the fatty acyl chain is indeed moving around relatively freely in the binding pocket, then there would be less loss in configurational entropy than one would have expected to attend protein binding of the highly flexible, free fatty acid. Measurements of the thermodynamics of fatty acid binding to I-FABP have shown the process to be enthalpically driven, and generally but not always entropically opposed (*16*, *39*).

As a last point, although not precisely analogous, the results shown here suggest that one should be cautious in interpreting apparent motional parameters of macromolecules when the "probe" being studied is apparently very mobile, i.e., the probe displays substantial "local" or segmental motion. The term segmental motion is commonly used, but there are seldom quantitative data available to allow precise definition of the meaning of the term. "Segmental mobility" is employed particularly frequently to describe the apparent mobility of fluorescent probes covalently attached to proteins. Unquestionably, motional parameters recovered, e.g., from fluorescence anisotropy decay data, must contain information on both the protein's and the probe's motion, but the values are often so convolved as to be inseparable in a sensible manner. The latter judgment is likely to be valid particularly when values recovered for the macromolecule's apparent rotational correlation time are substantially less than expected, other issues such as probe orientation and macromolecular shape dysymmetry (implying anisotropic overall molecular motion) notwithstanding. The model outlined here represents a framework for interpretation of NMR relaxation data when segmental motion is demonstrably present. Quantitative interpretation rests upon the validity of certain assumptions given above, but even if those are not met, the qualitative interpretation is still informative.

Summary. Palmitic acid showed a varied range of dynamics; the dynamics were the least restricted in micelles and in methanol solution, and most restricted in the complex of PA with I-FABP as reflected in the order parameter values. Within the PA·I-FABP complex, the mobility of the fatty acid was smallest, but nonetheless substantial, near the headgroup and largest at the acyl chain terminus. The fatty acid also appeared to undergo "segmental" motions within the protein binding cavity as indicated by our observation of an apparent effective overall correlation time for the complex that is smaller than that of the holoprotein. It will be of interest to learn if similar motional flexibility is present in other protein−ligand complexes.

ACKNOWLEDGMENT

We acknowledge Vladimir Likić of the Mayo Graduate School for preparing Figure 1 and for providing us information regarding dimensions of the I-FABP binding cavity. We thank Drs. Durgu Rao and Bruce Ray at the IUPUI NMR Center for advice and technical assistance. We thank Dr. Art Palmer of Columbia University for the computer program used for analysis of the NMR relaxation data.

REFERENCES

1. Kurian, E., Kirk, W. R., and Prendergast, F. G. (1996) *Biochemistry 35*, 3865−3874.
2. Veerkamp, J. H., Peeters, R. A., and Maatman, R. G. H. J. (1991) *Biochim. Biophys. Acta 1081*, 1−24.
3. Banaszak, L., Winter, N., Xu, Z., Bernlohr, D. A., Cowan, S., and Jones, T. A. (1994) *Adv. Protein Chem. 45*, 89−151.
4. Sacchettini, J. C., Gordon, J. I., and Banaszak, L. J. (1989) *J. Mol. Biol. 208*, 327−339.
5. Sacchettini, J. C., Gordon, J. I., and Banaszak, L. J. (1989) *Proc. Natl. Acad. Sci. U.S.A. 86*, 7736−7740.
6. Scapin, G., Gordon, J. I., and Sacchettini, J. C. (1992) *J. Biol. Chem. 267*, 4253−4269.
7. Sacchettini, J. C., Scapin, G., Gopaul, D., and Gordon, J. I. (1992) *J. Biol. Chem. 267*, 23534−23545.
8. Eads, J., Sacchettini, J. C., Kromminga, A., and Gordon J. I. (1993) *J. Biol. Chem. 268*, 26375−26385.
9. Hodsdon, M. E., and Cistola, D. P. (1997) *Biochemistry 36*, 1450−1460.
10. Hodsdon, M. E., Ponder, J. W., and Cistola, D. P. (1996) *J. Mol. Biol. 264*, 585−602.
11. Palmer, A. G. (1997) *Curr. Opin. Struct. Biol. 7*, 732−737.
12. Kay, L. E. (1998) *Nat. Struct. Biol. 5*, 513−517.
13. Chen, C., Feng, Y., Short, J. H., and Wand, A. J. (1993) *Arch. Biochem. Biophys. 306*, 510−514.
14. Pauls, K. P., Mackay, A. L., and Bloom, M. (1983) *Biochemistry 22*, 6101−6109.
15. Hamilton, J. A., Cistola, D. P., Morrisett, J. D., and Sparrow, J. T. (1984) *Proc. Natl. Acad. Sci. U.S.A. 81*, 3718−3722.
16. Kirk, W. R., Kurian, E., and Prendergast, F. G. (1996) *Biophys. J. 70*, 69−83.
17. Shaka, A. J., Keeler, J., Frenkiel, T., and Freeman, R. (1983) *J. Magn. Reson. 52*, 335−338.
18. Boyd, J., Hommel, U., and Campbell, I. D. (1990) *Chem. Phys. Lett. 175*, 477−482.
19. Zhu, L., Kemple, M. D., Landy, S. B., and Buckley, P. (1995) *J. Magn. Reson. B 109*, 19−30.

20. Kay, L. E., and Torchia, D. A. (1991) *J. Magn. Reson. 95*, 536−547.
21. Mandel, A. M., Akke, M., and Palmer, A. G (1995) *J. Mol. Biol. 246*, 144−163.
22. Kemple, M. D., Buckley, P., Yuan, P., and Prendergast, F. G. (1997) *Biochemistry 36*, 1678−1688.
23. Lipari, G., and Szabo, A. (1982) *J. Am. Chem. Soc. 104*, 4546−4559.
24. Tjandra, N., Feller, S. E., Pastor, R. W., and Bax, A. (1995) *J. Am. Chem. Soc. 117*, 12562−12566.
25. Clore, G. M., Szabo, A., Bax, A., Kay, L. E., Driscoll, P. C., and Gronenborn, A. M. (1990) *J. Am. Chem. Soc. 112*, 4989−4991.
26. Yuan, P., Fisher, P. J., Prendergast, F. G., and Kemple, M. D. (1996) *Biophys J. 70*, 2223−2238.
27. Lipari, G., and Szabo, A. (1982) *J. Am. Chem. Soc. 104*, 4559−4570.
28. Farrow, N. A., Muhandiram, R., Singer, A. U., Pascal, S. M., Kay, C. M., Gish, G., Shoelson, S. E., Pawson, T., Forman-Kay, J. D., and Kay, L. E. (1994) *Biochemistry 33*, 5984−6003.
29. Hodsdon, M. E., and Cistola, D. P. (1997) *Biochemistry 36*, 2278−2290.
30. Frolov, A., and Schroeder, F. (1997) *Biochemistry 36*, 505−517.
31. Haberland, M. E., and Reynolds, J. A. (1975) *J. Biol. Chem. 250*, 6636−6639.
32. Bengsch, E., Perly, B., Deleuze, C., and Valero, A. (1986) *J. Magn. Reson. 68*, 1−13.
33. Breslauer, K. J., Terrin, B., and Sturtevant, J. M. (1974) *J. Phys. Chem. 78*, 2363−2366.
34. Macdonald, P. M., McDonough, B., Sykes, B. D., and McElhaney, R. N. (1983) *Biochemistry 22*, 5103−5111.
35. Parmer, Y. I., Gorrissen, H., Wassall, S. R., and Cushley, R. J. (1985) *Biochemistry 24*, 171−176.
36. Lafleur, M., Fine, B., Sternin, E., Cullis, P. R., and Bloom, M. (1989) *Biophys. J. 56*, 1037−1041.
37. Kinosita, K. S., Kawato, S., and Ikegami, A. (1997) *Biophys. J. 20*, 289−305.
38. Kemple, M. D., Yuan, P., Nollet, K. E., Fuchs, J. A., Silva, N., and Prendergast, F. G. (1994) *Biophys. J. 66*, 2111−2126.
39. Richieri, G. V., Ogata, R. T., and Kleinfeld, A. M. (1995) *J. Biol. Chem. 270*, 15076−15084.
40. Kraulis, P. J. (1991) *J. Appl. Crystallogr. 24*, 946−950.

BI982087V